Cell Stem Cell
Article

Self-Formation of Optic Cups and Storable Stratified Neural Retina from Human ESCs

Tokushige Nakano,[1,2,4,5] Satoshi Ando,[1,2,4] Nozomu Takata,[1] Masako Kawada,[1] Keiko Muguruma,[1] Kiyotoshi Sekiguchi,[6] Koichi Saito,[4] Shigenobu Yonemura,[3] Mototsugu Eiraku,[1,2] and Yoshiki Sasai[1,2,5,*]
[1]Organogenesis and Neurogenesis Group
[2]Division of Human Stem Cell Technology
[3]Electron Microscopy Laboratory
RIKEN Center for Developmental Biology, Kobe 650-0047, Japan
[4]Environmental Health Science Laboratory, Sumitomo Chemical Co., Ltd., Osaka 554-8558, Japan
[5]Department of Medical Embryology, Graduate School of Medicine, Kyoto University, Kyoto 606-8501, Japan
[6]Laboratory of Extracellular Matrix Biochemistry, Institute for Protein Research, Osaka University, Suita 565-0871, Japan
*Correspondence: yoshikisasai@cdb.riken.jp
DOI 10.1016/j.stem.2012.05.009

SUMMARY

In this report, we demonstrate that an optic cup structure can form by self-organization in human ESC culture. The human ESC-derived optic cup is much larger than the mouse ESC-derived one, presumably reflecting the species differences. The neural retina in human ESC culture is thick and spontaneously curves in an apically convex manner, which is not seen in mouse ESC culture. In addition, human ESC-derived neural retina grows into multilayered tissue containing both rods and cones, whereas cone differentiation is rare in mouse ESC culture. The accumulation of photoreceptors in human ESC culture can be greatly accelerated by Notch inhibition. In addition, we show that an optimized vitrification method enables en bloc cryopreservation of stratified neural retina of human origin. This storage method at an intermediate step during the time-consuming differentiation process provides a versatile solution for quality control in large-scale preparation of clinical-grade retinal tissues.

INTRODUCTION

Complex organs such as the eye consist of many different kinds of cells that are integrated in a spatially restricted manner. Much progress has been made over the last decade in understanding the molecular mechanism of cellular differentiation, enabling in vitro generation of retinal cells, including photoreceptors and retinal pigment epithelium, from pluripotent stem cells (Boucherie et al., 2011; Lund et al., 2006; Lu et al., 2009a; Meyer et al., 2011; Osakada et al., 2008; Idelson et al., 2009; Lamba et al., 2006, 2010; Carr et al., 2009; Ikeda et al., 2005; Kawasaki et al., 2002). In contrast, little is known about the control of the complex 3D shape and pattern in retinal development.

We recently reported the formation of a 3D retina from mouse ESC (mESC) aggregates (Eiraku et al., 2011) using a versatile floating culture in serum-free and growth-factor-reduced medium (SFEBq culture, or serum-free culture of embryoid body-like aggregates with quick aggregation; Wataya et al., 2008; Eiraku et al., 2008). In SFEBq culture, mESCs spontaneously form a hollow vesicle of continuous neuroepithelium that differentiate into rostral forebrain tissues that include the retina-forming field. In particular, a modified SFEBq culture using Matrigel in low-growth-factor medium efficiently steers mESCs not only to differentiate into retinal progenitors, but also to form a two-walled cup-like structure mimicking the embryonic optic cup (Eiraku et al., 2011) (Figures S1A and S1B available online). Importantly, the optic cup formation is driven by self-organization; it spontaneously occurs via an intrinsic program of orchestrated local cellular interactions in a simple culture starting with the aggregation of mESCs in homogenous culture medium.

During early embryogenesis, the retinal anlage first appears as the optic vesicle, an epithelial vesicle evaginating laterally from the diencephalon. Subsequently, its distal portion invaginates to form the optic cup. The outer wall develops into retinal pigment epithelium (RPE), while the inner wall forms the neurosensory layers called neural retina (NR) (Graw, 2010). The optic cup generated in the modified SFEBq culture has RPE and NR epithelium with the correct topology, and the shape of the cup develops without the influence of external structures (Eiraku et al., 2011).

Furthermore, the mESC-derived NR epithelium, when isolated and cultured in suspension for additional 2 weeks, grows into a stratified NR tissue with six kinds of NR cells (photoreceptors, bipolar cells, ganglion cells, horizontal cells, amacrine cells, and Müller cells) aligned in multiple layers as seen in the postnatal eye (Eiraku et al., 2011). The formation of the stratified NR tissue is another example of self-organization in mESC culture; this multilayered structure spontaneously emerges from monolayered NR epithelium. Thus, this SFEBq culture enables the self-formation of the highly ordered 3D retinal pattern from patternless aggregates of mESCs in vitro (Eiraku et al., 2011; Ali and Sowden, 2011).

In the present study, we demonstrate that the optic cup structure and stratified NR also form from hESCs in a self-organizing manner. We also discuss some intriguing differences between mESC- and hESC-derived retinal tissues in the size, epithelial deformation mechanics, rod-versus-cone differentiation, and developmental speed.

RESULTS

Efficient Generation of Retinal Progenitors from hESCs in 3D Culture

In mESC culture, self-organized optic cup formation was most frequently seen when the culture contained a high percentage of retinal progenitors (typically 35%–70%). We therefore optimized retinal differentiation using hESC lines with *venus* cDNA knocked in at the locus of the early retina marker gene *Rx* (also called *RAX*; Mathers et al., 1997) (Figures S1C and S1D).

SFEBq culture was started by reaggregating dissociated hESCs in a low-cell-adhesion 96-well plate (9,000 cells/well) and was continued in serum-free differentiation medium (Figure S1E). Unlike mESCs, reaggregation of hESCs is slow and often incomplete when they are cultured in serum-free medium using a conventional U-bottomed well; in such conditions, the aggregates tend to vary in size, causing substantial variance in differentiation efficiency. This problem was largely solved by using a newly designed V-bottomed 96-well plate (conical-shaped; see Experimental Procedures), in which the aggregation was facilitated by the pointed bottom (Figure S1F).

One key for the efficient retinal differentiation in our previous mESC study was to reduce the concentration of knockout serum replacement additive (KSR; usually used at 10%–20%) in the medium to 1.5%–2%. However, hESCs inefficiently formed retinal epithelium at such low KSR concentrations in SFEBq culture (data not shown). A high KSR concentration tends to cause moderate caudalization in ESC-derived neural progenitors (data not known); this is not helpful for retinal differentiation, which occurs in the rostral diencephalon in vivo. Therefore, we counteracted the caudalizing activity of high KSR by treating the culture with a Wnt inhibitor (Lu et al., 2009b), which is known to have a rostralizing effect, during the early culture phase. In addition, to avoid dissociation-induced apoptosis, we added a ROCK inhibitor (Y-27632) to the SFEBq culture of hESCs, as we reported previously (Watanabe et al., 2007; Ohgushi et al., 2010).

Thus, we cultured hESC aggregates in 20% KSR-containing medium supplemented with the Wnt inhibitor IWR1-endo (IWR1e), Y-27632, and Matrigel for the first 12 days (Figure 1A). Then, we examined the effects of various signaling modulators on retinal differentiation by adding them to medium on day 12. One effective enhancer of retinal differentiation turned out to be fetal bovine serum (FBS; 10%) (Figure S1H). In addition, in the presence of FBS, treatment with the Hedgehog agonist smoothened agonist (SAG; 100 nM) augmented retinal differentiation in SFEBq culture of hESCs such that the proportion of Rx::venus$^+$ cells reached >70% of total cells (Figures 1B, 1C, and S1G; the majority of venus$^-$ tissues were N-cadherin$^+$ and Sox2$^+$ neural progenitors; Figures S1I and S1J).

Self-Formation of Optic Cups in 3D hESC Culture

Importantly, most of the retinal epithelium generated under the Matrigel+IWR1e+FBS+SAG (MIFS) conditions was positive for Chx10 (NR progenitor marker; Liu et al., 1994) and Pax6, and negative for the RPE marker Mitf (Martínez-Morales et al., 2004) (Figures 1D–1K). This indicates that the induced retinal epithelium preferentially differentiated into NR epithelia in this culture (NR-selective culture, hereafter).

We therefore searched for RPE-generating culture conditions. We first examined the effect of prolonged treatment with FBS (days 12–21), which is known to support the growth of RPE (Kawasaki et al., 2002), but did not observe any substantial RPE-inducing effects (data not shown; instead, prolonged FBS treatment enhanced the formation of continuous NR epithelia; Figures 1L and 1M). In contrast, treatment with the Wnt agonist CHIR99021 (GSK3β inhibitor) during days 18–21 efficiently induced the formation of large thin epithelia expressing Mitf (Figures 1N and 1O; indeed, further culture of these aggregates developed RPE with massive pigmentation; Figures 1P and 1Q) and inhibited NR differentiation (data not shown). The RPE-inducing effect of Wnt signaling (when added after the cells are committed to the retinal fate) is consistent with previous reports of in vivo mouse studies (Fuhrmann, 2008; Westenskow et al., 2009; Liu et al., 2010; Fujimura et al., 2009) and our previous in vitro mESC study.

The formation of the optic cup structure needs both NR and RPE tissues in a balanced fashion. For this balance, the temporal window of the Wnt agonist treatment was critical, and the addition of CHIR99021 to medium during days 15–18 substantially increased *Mitf* expression, without suppressing *Chx10* expression (Figures 2A, 2B, and S2A). Under these conditions (SFEBq/MIFS+W, hereafter), Rx::venus$^+$ epithelia appeared as patches on day 12 and subsequently underwent characteristic retinal morphogenesis, evaginating to form optic-vesicle-like structures (found in 58%–73% of aggregates; four experiments, 96 aggregates per experiment; Figures 2C and S2B and Movie S1).

The Chx10$^+$ distal portion of the hESC-derived retinal epithelium at this stage already exhibited a morphological characteristic of early pseudostratified epithelium (Figure 2D). Live imaging showed that the cells in the distal epithelium of the hESC-derived optic vesicle were highly proliferative and underwent interkinetic nuclear migration, typical for pseudostratified epithelium (Norden et al., 2009) (Figures 2E and 2F and Movie S2).

During days 19–24, the distal portion of the vesicle bent inwards (invagination), forming a double-walled optic cup structure (Figures 3A–3C and S3A–S3C and Movie S3; found in 21%–24% of SFEBq/MIFS+W aggregates; five experiments; 96 aggregates per experiment). As in vivo, while the thick inner portion expressed Chx10 (Figure 3D, blue; n = 30), the outer epithelium expressed Mitf (Figure 3D, red) and gradually started moderate pigment accumulation (Figure S3C, arrowheads). As with the mESC culture, there were no external structures pushing the tissue inwards such as lens or surface ectoderm, suggesting that the invagination of hESC-derived NR was self-driven by an intrinsic program within the retinal epithelium.

As seen in the embryonic retina (Hilfer and Yang, 1980), the pseudostratified NR epithelium was tall, and the RPE epithelium

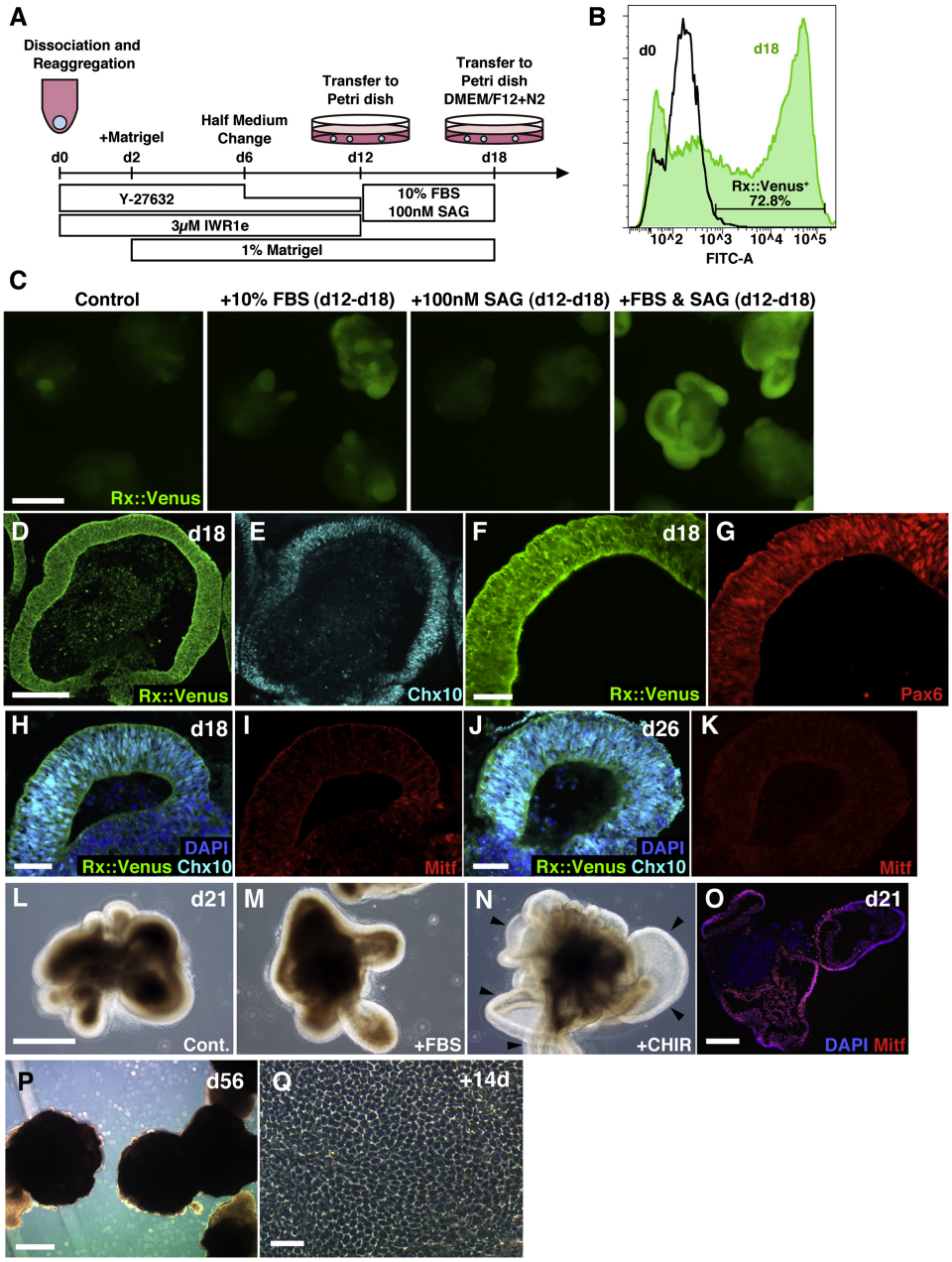

Figure 1. Optimized Generation of Retinal Epithelia in 3D hESC Culture

(A) Schematic of NR-selective SFEBq culture of hESCs.

(B) FACS analysis of Rx::venus$^+$ cell population on day 18 (green). Black, control undifferentiated *Rx::venus* hESCs. Reproducible results were obtained from three independent studies.

(C) Positive effects of FBS and SAG (added during days 12–18) on Rx::venus$^+$ retinal epithelial formation.

(D–I) Immunostaining of day-18 Rx::venus$^+$ epithelia generated from hESCs in NR-selective SFEBq culture. Stains are for GFP (D, F, and H; green), Chx10 (E and H; light blue), Pax6 (G; red), and Mitf (I; red; no substantial expression). Dark blue, nuclear staining with DAPI (H).

(J and K) Immunostaining of day-26 Rx::venus$^+$ epithelia. Stains are for GFP (J; green), Chx10 (J; light blue) and Mitf (K; red). Dark blue, nuclear staining with DAPI (J). The RPE maker was not expressed in the retinal epithelia generated under these conditions, even at this late stage.

(L–O) Additional treatment of day-18 retinal epithelia (generated as in A) with CHIR99021 (N and O) but not with FBS (M and not shown) during days 18–21 induced thin epithelia (N; arrowheads) with Mitf expression (O) on day 21. Bright-field views (L–N) and Mitf immunostaining are shown on a cryosection (O; red). Dark blue, nuclear staining with DAPI (O).

(P and Q) Example of massive pigmentation was seen after longer culture in the day-56 SFEBq aggregates treated with CHIR99021 (during days 18–25). 10% FBS and 50 ng/ml Activin were added to culture medium during days 18–56 and days 18–25, respectively. When these pigmented tissues were replated on the culture dish and cultured for additional 14 days, cells exhibited polygonal morphology typical for RPE (Q).

Scale bars: 500 μm (C, L, and P); 200 μm (D and O); 50 μm (F, H, J, and Q). See also Figure S1.

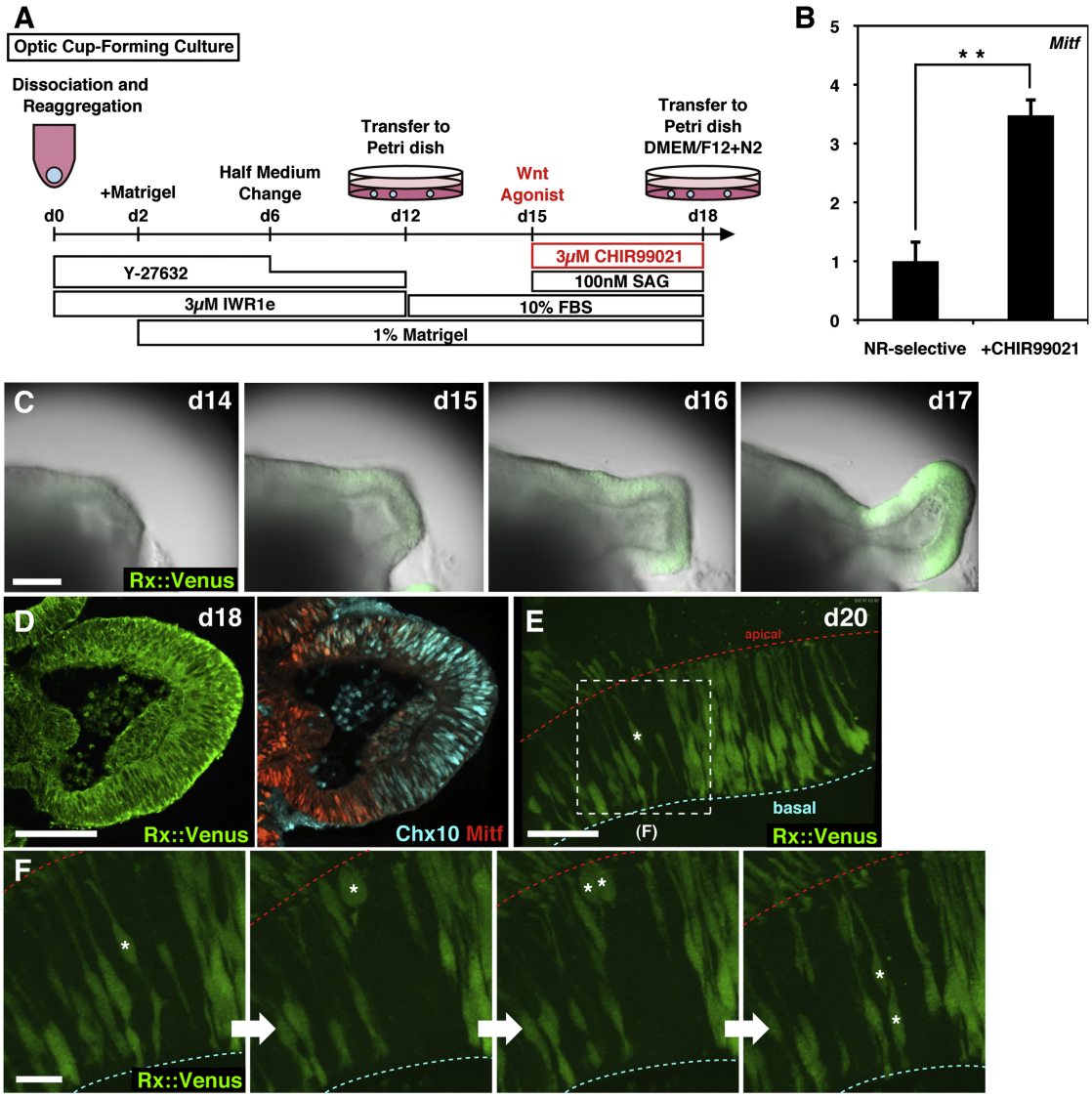

Figure 2. Self-Organized Formation of Optic Vesicles from hESC-Derived Retinal Epithelium

(A) Schematic of optic-cup-forming SFEBq culture of hESCs. The effects of SAG treatment during days 15–18 on the retinal formation were similar (not shown).

(B) Additional treatment with CHIR99021 during days 15–18 promoted *Mitf* expression in qPCR analysis (n = 3 experiments; each experiment with 12 aggregates). **p < 0.01, Students' t test.

(C) Live imaging of self-formation of an optic vesicle (Rx::venus$^+$) evaginating from hESC-derived retinal epithelium cultured under the conditions of (A).

(D) Immunostaining of Chx10 (right; light blue) and Mitf (right; red) in the day-18 Rx::venus$^+$ optic vesicle (left; the same section). Chx10 expression and Mitf expression were found in the distal and proximal portions of the retinal epithelium.

(E and F) Time-lapse multiphoton images showing interkinetic nuclear migration of retinal progenitors in the day-20 optic-vesicle epithelium. Cells were attracted toward the apical surface (red line) and underwent proliferation. The square region in (E) corresponds to the region in (F). Partial labeling of cells was done by mixing the venus-reporter cells with nonlabeled hESCs at reaggregation.

**p < 0.01; error bars show SEM. Scale bars: 200 μm (C); 100 μm (D); 50 μm (E); 20 μm (F). See also Figure S2 and Movie S1 and Movie S2.

was shorter (Figures 3D–3F). The hinge epithelium, which connects the NR and RPE tissues at an angled joint, formed a wedge-shaped domain with a very small apical area (Figure 3G). The appearance of the wedge-shaped hinge epithelium could be traced back to day 17 (Figure 3H; 100%, n = 15), when the optic vesicle epithelium started to make a visible flexure (Figure 2C). The aPKC$^+$ apical surface was inside, and the laminin-accumulating basal end was outside (Figure 3I; 100%, n = 20). A notable domain-specific mechanical property found in the mESC-derived optic cup is that its NR has a very low level of myosin activity (as shown by low pMLC2 levels), while the RPE contains high levels of pMLC2, particularly on the apical side (Eiraku et al., 2011, 2012). This makes the NR much less stiff than the RPE. A similar situation of region-specific actomyosin

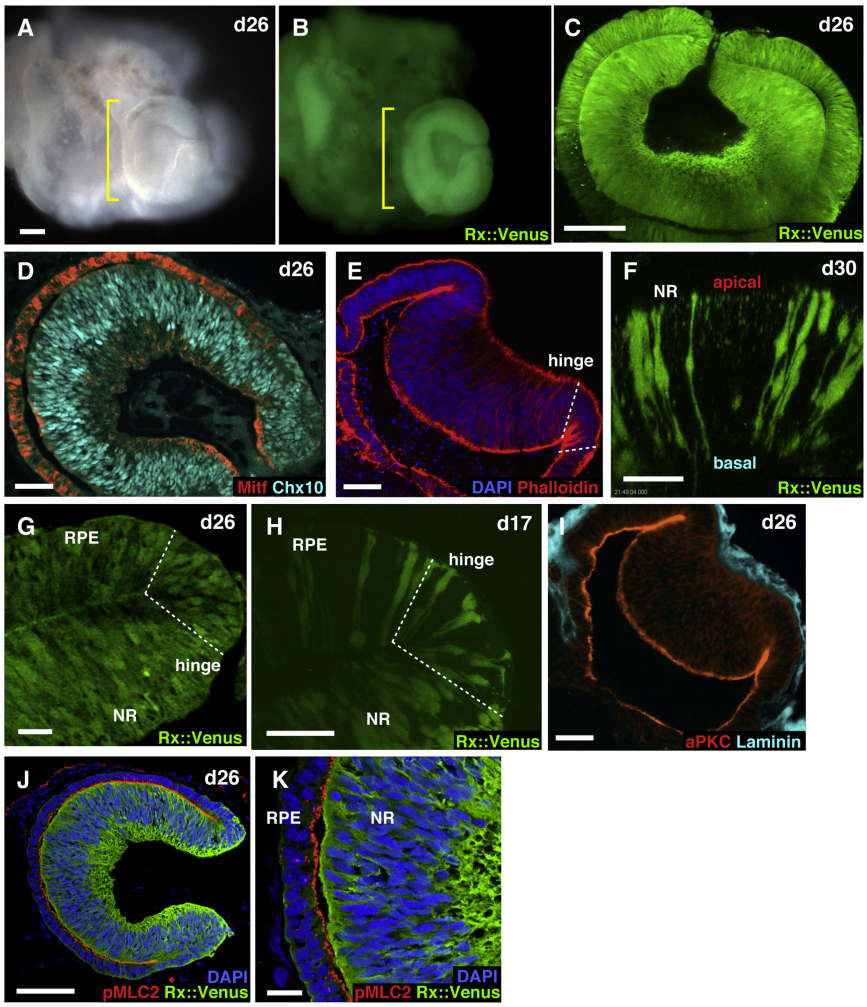

Figure 3. Self-Organized Formation of Optic Cups from hESCs

(A and B) Low-magnification views of the day-26 optic cup (yellow bracket) formed in the hESC aggregate. (A), bright-field view; (B), fluorescence image.

(C) Optical cross-section of the day-26 optic cup by multiphoton imaging.

(D) Immunostaining of the day-26 optic cup for Chx10 (light blue) and Mitf (red).

(E) Phalloidin (red) and DAPI (dark blue) staining of the day-26 optic cup. The hinge region was indicated by broken lines.

(F) Elongated morphology of progenitors in the pseudostratified NR epithelium on day 30. Multiphoton image. Partial labeling of cells was done by mixing the venus-reporter cells with nonlabeled hESCs at reaggregation.

(G) High-magnification image of Rx::venus expression in the hinge region of the day-26 optic cup.

(H) Wedge-like shape of the hinge region in the day-17 optic vesicle generated from hESCs. Partial labeling of cells was done by cell mixing as above.

(I) Immunostaining of the day-26 optic cup for aPKC (apical; red) and Laminin (basement membrane; light blue).

(J and K) Immunostaining of the day-26 optic cup (Rx::venus^{+}; green) for phospho-MLC2 (pMLC2; red) (K is a high-magnification view). In the optic cup, pMLC2 was strongly accumulated on the apical side of the RPE, but not substantially observed in the NR.

Scale bars: 100 μm (A, B, C, I, and J); 50 μm (D and E); 40 μm (F and H); 20 μm (G and K). See also Figure S3.

control was seen in the hESC-derived optic cup; a substantial accumulation of pMLC2 was observed in the RPE but not in the NR (Figures 3J and 3K).

Taken together, these findings indicate that hESC-derived retinal epithelium spontaneously forms an optic cup structure by self-organization, as has been reported for mESC culture.

Structural and Morphogenetic Differences between hESC and mESC Cultures

Although the self-organizing formation of optic cup structures occurs in both mESC and hESC cultures, there are several intriguing differences between them. First, the developmental process took much longer than in mESC culture (e.g., optic cup formation took ~24 days and ~9 days in hESC and mESC culture, respectively). Second, the early optic cups generated from hESCs were substantially bigger (initially ~550 μm in long-axis diameter; Figures 4A and 4B) than those from mESCs (initially ~250–300 μm; Eiraku et al., 2011; see Figure S1A). The hESC-derived NR was also substantially thicker (120–150 μm; Figure 4C) than the mESC-derived NR in the early optic cup (60–80 μm; Figure S1A). These observations are in accord with the differences seen in the human and mouse optic cups during early retinogenesis; the early human optic cup at Carnegie stage 15, or fetal day 35, is ~500 μm in diameter (O'Rahilly and Müller, 1999), whereas the mouse optic cup on embryonic day 10–10.5 is around 250 μm (Figure S1B).

In theory, the infolding of the thick epithelia-like hESC-derived NR should require more mechanical elaboration than that of the thinner one from mouse cells. In this respect, we found another intriguing difference in the deformation mechanics between hESC and mESC cultures. Whereas the early retinal epithelia before invagination were apically concave (Figure 4D; Eiraku et al., 2011), the NR epithelia after invagination became apically convex in both hESC and mESC cultures. This direction of curving was fixed at this stage, and maintained even when the NR epithelia were isolated from the main body of the aggregates (Figure S4A). Our previous study demonstrated that the NR eversion (from apically concave to convex) in mESC culture requires the presence of RPE and the hinge (Eiraku et al., 2012) and does not spontaneously occur in NR epithelium isolated before invagination (Figure 4D, top; Eiraku et al., 2011). In contrast, the hESC-derived NR epithelia, when isolated on day 18, gradually underwent spontaneous eversion and became apically convex over the next few days (100%, four experiments; 20 aggregates per experiment; Figures 4D–4F and Movie S4), regardless of culture conditions before isolation

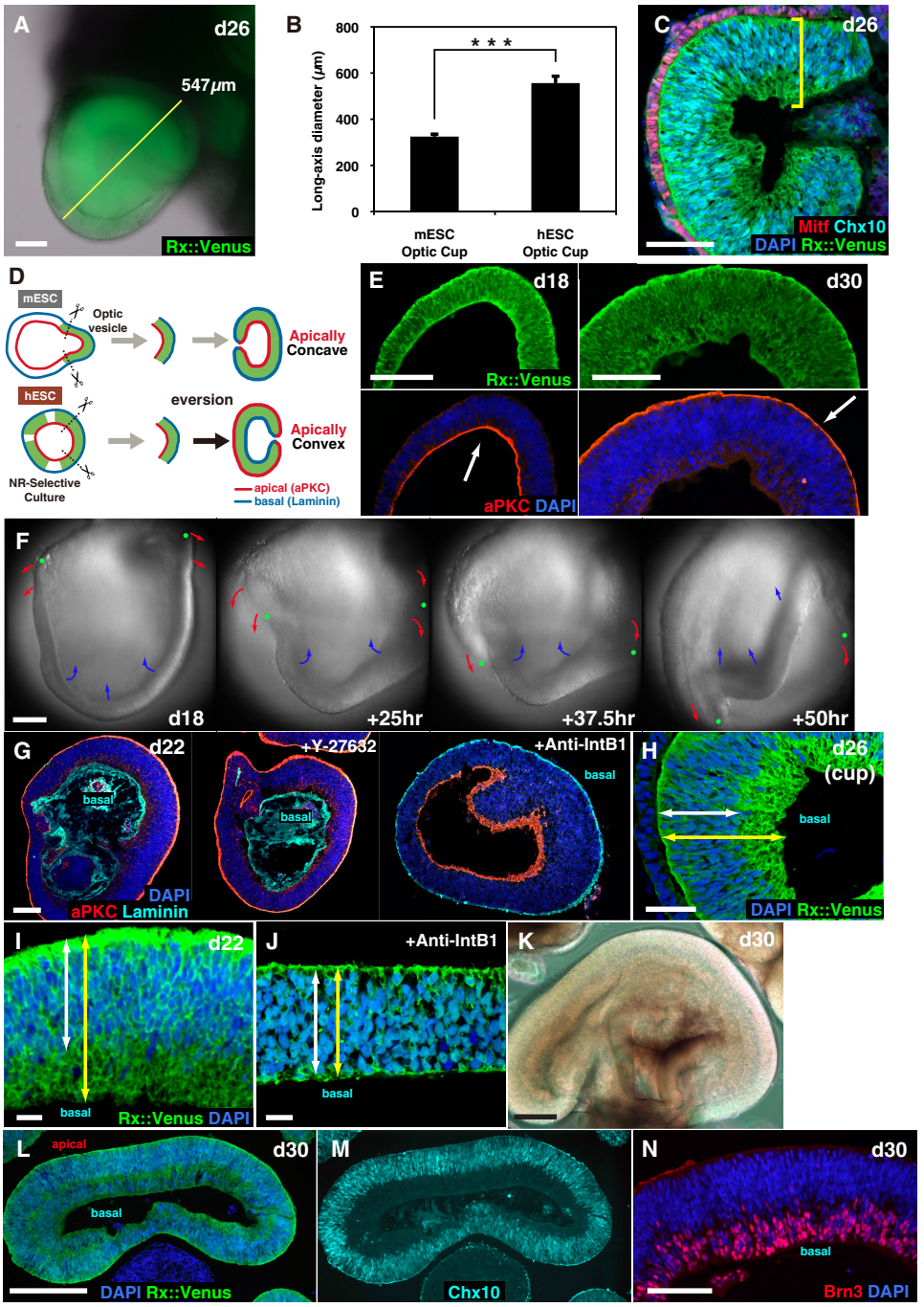

Figure 4. Optic Cup Features Specific to hESC Culture

(A and B) Size measurement of the day-26 optic cup. (A) The long and short axes were always perpendicular (yellow line) and parallel to the central axis of the cup (NR center to the center of the cup opening), respectively (n = 20). (B) Long-axis diameters of the day-26 optic cups derived from hESCs (n = 8 cups), compared with those of mESC-derived day-9 optic cups (n = 8). ***p < 0.001, Student's t test.

(C) Thick NR epithelium (yellow bracket) in the hESC-derived day-26 optic cup.

(D) Schematic of the NR eversion, which occurs in the isolated retinal epithelia of hESC culture (excised on day 18; before invagination), but not in those of mESC culture (excised on day 7; before invagination).

(E) Apical-basal eversion of hESC-derived NR epithelia excised from SFEBq aggregates generated under the NR-selective conditions. Left and right panels show hESC-derived NR epithelia on day 18 and day 30, respectively, in the isolation culture. The aPKC^{+} apical surface (red; bottom; shown by arrows) was inside on day 18 but outside on day 30.

(F) Live-imaging analysis of the eversion of NR epithelia excised on day 18. Green dots indicate cutting edges.

(G) Immunostaining of the day-22 NR (isolation culture from day 18) for aPKC (apical; red) and Laminin (basement membrane; light blue) with DAPI nuclear staining (dark blue). Left, control; middle, treated with the ROCK inhibitor Y-27632 (10 μM) during days 18–22; right, treated with anti-β1 integrin-neutralizing antibody

(SFEBq/MIFS±W). These findings suggest that the hESC-derived NR epithelium has an intrinsic tendency to bend in an apically convex manner, which can contribute to the infolding of this thick tissue during invagination.

The spontaneous apical eversion of hESC-derived NR was not sensitive to ROCK inhibitor, which blocks the Rho-myosin pathway. In contrast, the apical eversion was inhibited when integrin signaling was blocked by its neutralizing antibody (blocked in 75%, n = 24; see the reduced phospho-paxillin levels on the basal side; Figure S4C), suggesting an essential role of basement-membrane-mediated signals in this process. There were no substantial changes in proliferation (phosho-H3, Ki67) or apoptosis (active caspase 3) (Figures S4D and S4E). One obvious difference along the apical-basal axis of the NR was the positions of the nuclei (i.e., the location of the cell bodies of the radial-glia-like NR progenitors), which were strongly deviated to the apical side in hESC culture (Figure 4H). This strong deviation in cell position is also found in the human fetal optic cup (O'Rahilly and Müller, 1999), but not in the early mouse optic cup or the mESC-derived optic cup (e.g., Figures S1A and S1B; Eiraku et al., 2011). The apically biased localization of cell bodies can theoretically contribute to the preferential volume expansion on the apical side, potentially leading to the apically convex curvature in the NR. Interestingly, integrin blockade diminished the apical nuclear deviation within the hESC-derived NR (Figures 4I and 4J), along with the inhibition of the eversion, suggesting that both depend on some basement membrane signals.

Multilayered NR Containing Photoreceptors, Ganglion Cells, and Interneuron Precursors

Early NR tissues obtained from both NR-selective (Figure 1) and optic-cup-forming (Figure 2) cultures grew to form stratified tissues (in this report, we mainly show the results from the NR-selective culture below). When retinal epithelia were isolated en bloc (typically 300–500 μm in diameter) from day-18 SFEBq aggregates and cultured in suspension, the NR epithelia grew into larger epithelial vesicles and remained Rx::venus$^+$ on day 30 (Figures 4K and 4L; the long-axis diameter was typically ~1 mm). The great majority of cells in the day-30 NR were positive for the progenitor marker Chx10 (Figure 4M) and the mitotic marker Ki67 (not shown). In the embryo, NR epithelia generate several kinds of retinal components in a temporally controlled manner, with the first-born cell lineage being ganglion cell (Brn3$^+$/Pax6$^+$) (Mu and Klein, 2004; Cayouette et al., 2006). As in the embryonic eye, postmitotic ganglion cells began to emerge during early phases of hESC culture (around day 24; data not shown). Their number gradually increased over the next week, and formed a distinct layer at the basal-most zone of the hESC-derived NR (Figure 4N and data not shown).

We next investigated photoreceptor differentiation (Figure 5) using hESC lines with *venus* cDNA knocked in at the locus of the early photoreceptor marker gene *Crx* (Furukawa et al., 1997) (Figure S5A). On days 28–34, a relatively small number of Crx::venus$^+$ cells were present, most of which were found between the ganglion (Brn3$^+$) and the progenitor (Chx10$^+$) cell layers (hereafter referred to as the intermediate-deep zone) (Figure 5A and not shown). On day 42, in addition to the intermediate-deep layer, the apical layer of the NR also accumulated Crx::venus$^+$ cells (Figure S5B). The photoreceptor-precursor marker Blimp1 (Katoh et al., 2010; Brzezinski et al., 2010) was also expressed in these cells (Figure S5C). At this stage, TuJ1$^+$ axons of ganglion cells already formed bundles in the basal-most zone (Figure S5D).

On day 60, NR tissues became ~2 mm in long-axis diameter and ~200 μm in thickness. Despite this thickness, the NR tissue remained semitransparent (Figure 5B). Crx::venus$^+$ photoreceptors located in both the apical-most and intermediate-deep layers (Figure 5C) expressed the bona fide photoreceptor marker Recoverin (Figure S5E) and were negative for Ki67 (mitotic marker; Figure S5F). During days 42–60, Chx10$^+$ progenitors (Chx10$^+$, Ki67$^+$) still constituted the largest population in culture and formed a thick layer between the two Crx::venus$^+$ zones (not shown), while Brn3$^+$/Tuj1$^+$ ganglion cells were preferentially localized to the basal side (Figure S5G) as seen on day 42.

Later, on day 126 (thickness was >250 μm; Figure 5D), Crx::venus$^+$ photoreceptors in the apical-most layer further increased in number (12%–18% of total cells; n = 4; >1,000 cells for each) and were densely packed (Figure 5E). The apically located photoreceptors expressed not only Recoverin (Figure 5F), but also the rod-specific marker Nrl (Mears et al., 2001) or the early cone marker Rxr-gamma (Janssen et al., 1999; also expressed in ganglion cells) (Figures 5G and 5H). The ratio of Nrl$^+$ to Rxr-gamma$^+$ cells in the apical-most layer of the day-126 NR was 4.1 ± 1.6: 1 (n = 4; >200 cells for each). On the apical side, these photoreceptors formed ZO-1$^+$ tight junctions (Figure 5I, red) and substantially accumulated the visual pigments rhodopsin and color opsins (Figures 5J–5L, S5H, and S5I).

Chx10$^+$ progenitors were still found in the intermediate layer, while Tuj1$^+$ postmitotic neurons were found on the basal side (Figures 5M, 5N, and S5J). Ptf1a$^+$ interneuron precursors, becoming amacrine and horizontal cells later (Fujitani et al., 2006), were present mostly near the Crx::venus$^+$ cells in the intermediate-deep layer (Figure 5O). Calretinin$^+$ cells (marker for amacrine and ganglion cells) and GABA$^+$ neurons (Figures 5P, 5Q, and S5K) were also present in the intermediate-deep

(5 μg/ml) during days 18–22. In the controls and the Y-27632-treated groups (n = 20), all NR epithelia underwent apical-basal eversion, while the integrin-antibody-treated group remained apically concave (75%, n = 24; two independent experiments).

(H–J) Apically derived nuclear localization (white zone; dark blue, DAPI nuclear staining) in the Rx::venus$^+$ NR epithelium (yellow) of the day-26 optic cup (H) and day-22 NR (I). The anti-integrin antibody caused an even distribution of nuclear positions as seen in mESC-derived NR (J). (K) Semitransparent day-30 NR epithelium in isolation culture.

(L–N) Cross-sections of day-30 NR epithelia (forming a vesicle). Rx::venus expression was observed throughout the epithelium (L; green; dark blue, DAPI nuclear staining). Chx10$^+$ progenitors (light blue; the same section as L) were located preferentially in the apical (outer) zone (M). (N) Brn3$^+$ ganglion cells were located on the basal side.

***$p < 0.001$; error bars show SEM. Scale bars: 200 μm (K and L); 100 μm (A, C, E, F, G, and N); 50 μm (H); 20 μm (I and J). See also Figure S4 and Movie S4.

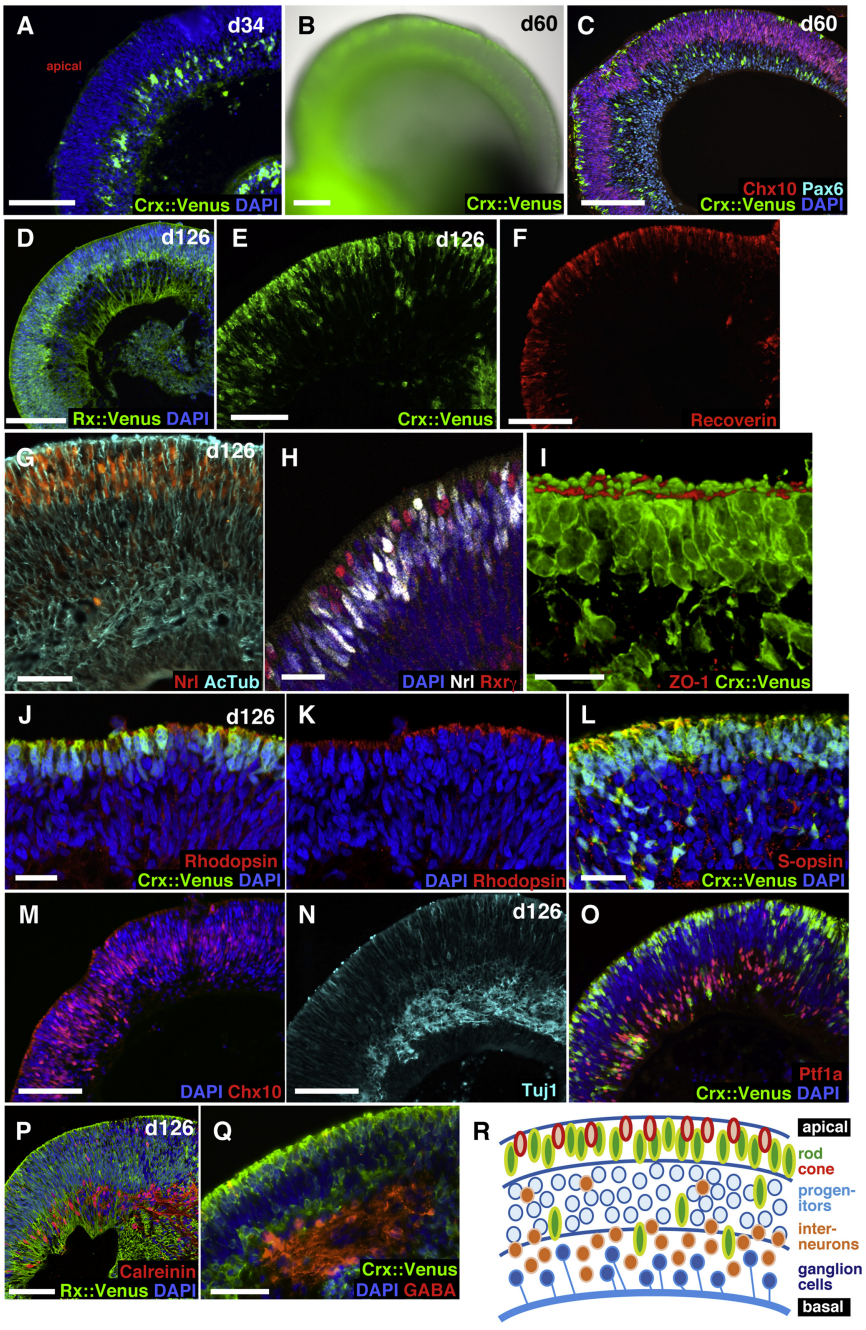

Figure 5. Self-Formation of Multilayered NR Tissue from hESCs

(A) A relatively small number of Crx$^+$ photoreceptor precursors were found in the intermediate-deep zone of the day-34 NR epithelium.

(B) Semitransparent NR epithelium on day 60. Crx::venus fluorescence from the inside of NR could be seen by external observation.

(C) Immunostaining of the day-60 NR epithelium for GFP (Crx::venus$^+$ photoreceptor precursors; green), Chx10 (progenitors; red), and Pax6 (strong staining in ganglion cells; light blue) with DAPI nuclear staining (dark blue).

(D–Q) Immunostaining of day-126 NR epithelia. The day-126 NR epithelium was thick (>250 μm; D). (E) Accumulation of Crx::venus$^+$ photoreceptor precursors on the apical-most zone. (F–L) The apical-most zone contained many recoverin$^+$ photoreceptors (F); some expressed the rod marker Nrl (red, G; white, H), and others expressed the cone marker Rxr-gamma (red, H). The apical photoreceptors formed ZO-1$^+$ apical junctions (I). The visual pigments rhodopsin (red, J and K) and S-opsin (red, L) were accumulated on the apical surface. (M and N) Chx10$^+$ NR-progenitors were present in the intermediate zone (M), while TuJ1$^+$ postmitotic neurons were mostly found in the more-basal domain (N). (O) Ptf1a$^+$ interneuron precursors (red) were found in the intermediate-deep and deep zones. (P and Q) Most of the calretinin$^+$ neurons (P) and GABA neurons (Q) were located in the basal zone near the intermediate-deep zone (basal Crx::venus$^+$ photoreceptor precursors).

(R) Schematic of multilayered NR generated from hESCs.

Scale bars: 200 μm (B–D); 100 μm (A, E, F, M, N, and P); 50 μm (G and Q); 20 μm (H–J and L). See also Figure S5.

and deep layers. In addition, a small number of calbindin$^+$ cells with immature features were found; unlike mature calbindin$^+$ horizontal cells (located near the apical photoreceptor layer and extending neurites horizontally), the majority of calbindin$^+$ cells in this culture were located near the basal zone, while some calbindin$^+$ cells in the intermediate zone were vertically long in shape (indicative of immaturity; Figures S5L and S5M).

Bipolar cells are late-born neurons in retinogenesis in vivo. Consistent with the idea, few postmitotic bipolar cells (PKC$^+$) were observed even at this stage (n = 20; not shown). Also in accordance with the lack of bipolar cells, PSD95$^+$ plexiform layers (synaptic zones) were not observed (n = 20; not shown). On day 126, outside of the apical junctions, the photoreceptors had apical protrusions of monociliated, mitochondria-rich cell bodies, reminiscent of inner segments (ellipsoids), which carry connecting cilia (Ishikawa and Yamada, 1969; Besharse and Insinna, 2010) (Figures S5N–S5P; some cilia had a membrane vesicle on their tips, but no obvious outer-segment formation was seen; Figure S5P, arrow).

Taken together, these findings demonstrate that hESC-derived retinal epithelium can spontaneously generate stratified fetal-like NR tissues containing multiple components in a spatially arranged manner (Figure 5R).

Slow Photoreceptor Generation Accelerated by Notch Inhibition

Unlike mESC culture, the number of photoreceptors (Crx::venus$^+$ precursors and Recoverin$^+$ cells) increased only gradually in hESC culture (over 13–18 weeks). However,

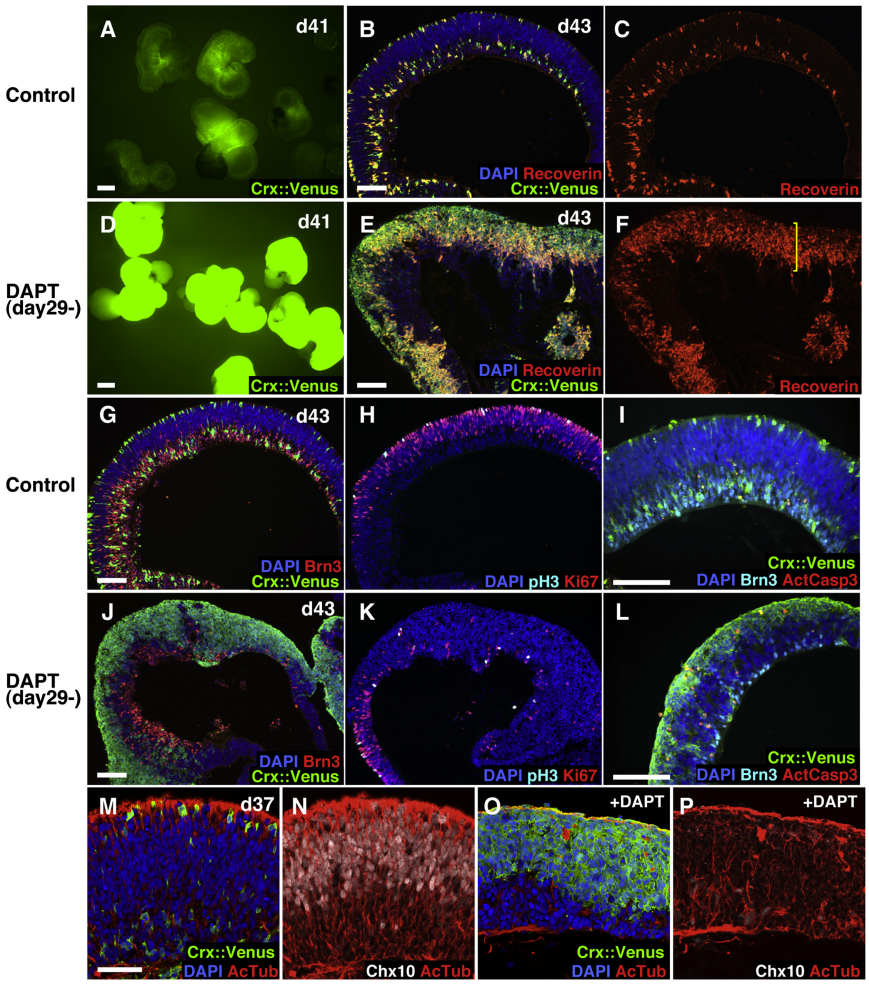

Figure 6. Accelerated Generation of Photoreceptors by Notch Inhibition

(A–C) Control NR epithelia (carrying *Crx::venus*), excised on day 19. (A) Crx::venus fluorescence on day 41. (B and C) Immunostaining of day-43 NR epithelia for Recoverin and Crx::venus (B).

(D–F) NR epithelia (carrying *Crx::venus*), excised on day 19 and treated with DAPT during days 29–43. (D) Crx::venus fluorescence on day 41. (E and F) Immunostaining of day-43 NR epithelia for Crx::venus (E) and Recoverin. Bracket, expanded photoreceptor layer (Crx^+/$Recoverin^+$).

(G–I) Immunostaining of control day-43 NR epithelia (carrying *Crx::venus*, excised on day 19) for GFP (green; G and I), Brn3 (red, G; light blue, I), Ki67 (red, H), pH3 (light blue, H), and active caspase 3 (red, I).

(J–L) Immunostaining of day-43 NR epithelia treated with 10 μM DAPT during days 29–43 for Crx::venus (J and L), Brn3 (J and L), Ki67 (K), pH3 (K), and active caspase 3 (L). (M and N) Immunostaining of control day-37 NR epithelia (carrying *Crx::venus*; excised on day 18) for acetylated tubulin (AcTub; red; M and N) and Chx10 (white, N; the same section as M). (O and P) Immunostaining of day-37 NR epithelia (carrying *Crx::venus*; excised on day 18) treated with DAPT during days 29–37 for AcTub (red; O and P) and Chx10 (white, P; the same section as O). Both Chx10 cells and the apical-basal arrangement of AcTub signals (indicative of the presence of radial glia-like progenitors) disappeared after DAPT treatment.

Scale bars: 500 μm (A and D); 100 μm (B, E, G, I, J, and L); 50 μm (M). See also Figure S6.

treatment of day-29 NR epithelia with the Notch inhibitor DAPT (Jadhav et al., 2006; Osakada et al., 2008) for 12–14 days dramatically increased the number of $Crx::venus^+$/$Recoverin^+$ photoreceptor cells (40%–78% of NR cells on day 43; Figures 6A–6F and S6A–S6F, and not shown), showing that a large portion of progenitors at this stage had the competence for photoreceptor differentiation (enhanced differentiation was already seen after 4 day DAPT treatment; Figures S6G–S6J). The number of $Brn3^+$ ganglion cells did not change dramatically (Figures 6G and 6J; 13%–19% of NR cells regardless of DAPT treatment; four experiments). In contrast, the number of mitotic progenitors ($Ki67^+$ cells) substantially decreased after the treatment (Figures 6H and 6K). There was a marginal increase in apoptosis (active $caspase3^+$) on day 43, but its level was only moderate (Figures 6I and 6L).

These findings indicate that photoreceptor differentiation in hESC culture is a slow process that is decelerated by Notch signaling but can be strongly accelerated by treatment with a Notch inhibitor. On day 43 (after 2 weeks of DAPT treatment), the NR epithelia became somewhat irregular in shape (Figures 6E and 6F). We infer that this was presumably tissue-architectural perturbation caused by the rapid loss of $Chx10^+$ retinal progenitors, which are structurally similar to radial glia in the developing cortex. Along with the accelerated differentiation into photoreceptors, the loss of progenitors occurred during the first several days of DAPT treatment (Figures 6M–6P).

Efficient En Bloc Cryopreservation of hESC-Derived NR Epithelium

The generation of stratified NR tissues takes much longer in hESC culture than in mESC culture, presumably reflecting the difference in gestational period between the two species (>260 days versus 20 days). It is technically challenging, however, to continue large-scale culture for more than several weeks in a row while controlling the product quality in a reproducible manner. To address this problem, we sought to develop an en bloc cryopreservation method that would enable the NR epithelia to be stored partway through the differentiation process. According to our observations, the most critical period for successfully generating stratified NR from hESCs is the first 30–40 days; NR that grew well up to this point tended to continue growing as a healthy-looking epithelium with multiple layers. Therefore, we aimed to develop an efficient cryopreservation method for storing the NR epithelia at this stage.

$Rx::venus^+$ NR tissues were isolated from SFEBq-cultured hESC aggregates on day 18 and cultured in suspension until

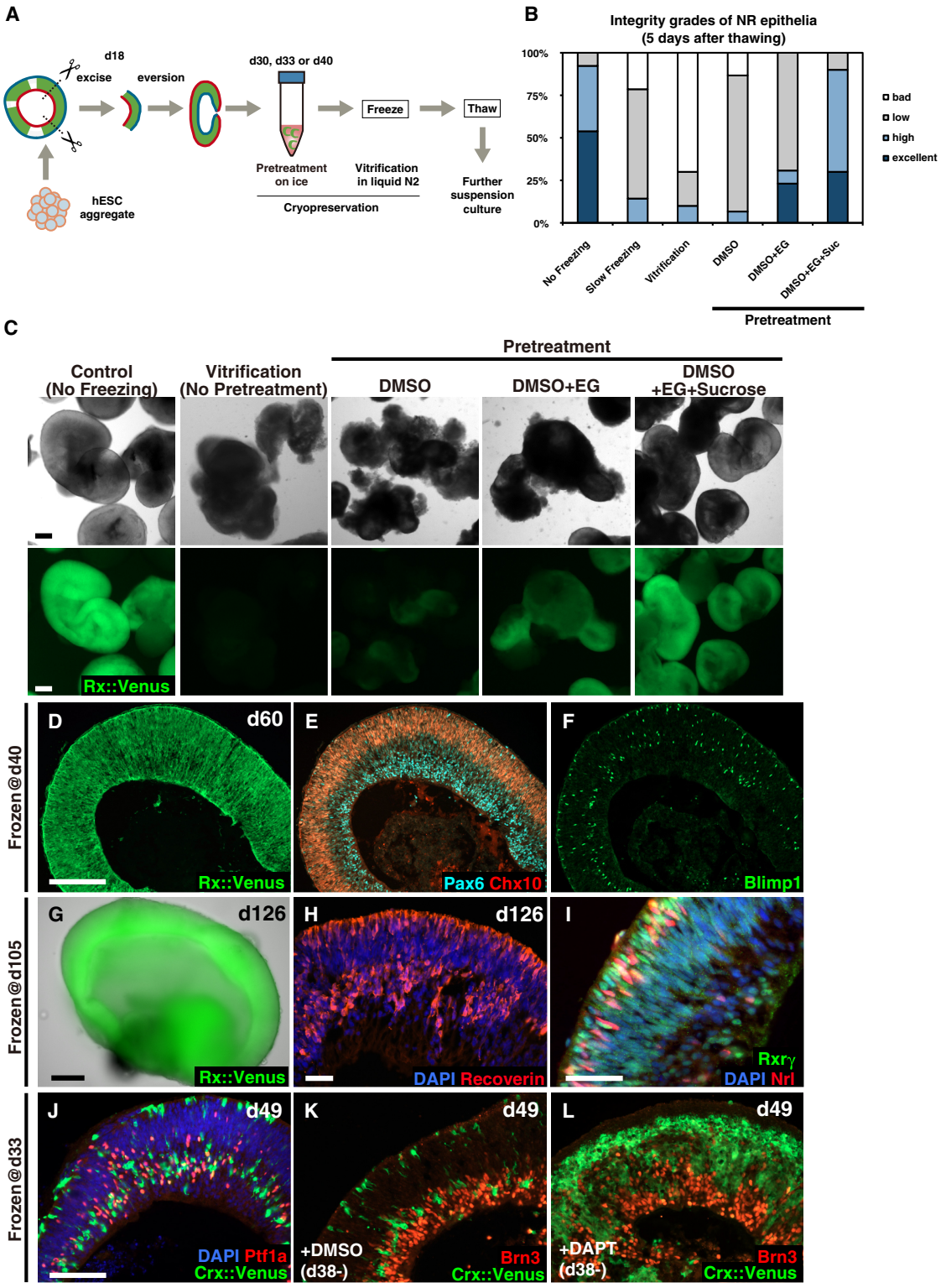

Figure 7. Efficient Cryopreservation of hESC-Derived NR Epithelia

(A) Schematic of the cryopreservation process.

(B) Semiquantitative comparison of different cryopreservation conditions for NR tissue survival (extent of epithelial integrity) 5 days after thawing (frozen on day 30; 15–20 NR epithelia/condition). Integrity of the epithelium of each vesicle: grade 1 (excellent), continuous smooth surface in >90% of the epithelial region; grade 2 (high), 50%–90%; grade 3 (low), 25%–50%; grade 4 (bad), less than 25%. Frequency of each grade found among the thawed NR epithelia is shown by percentage.

day 30. Then, the NR epithelia were subjected to cryopreservation en bloc under various conditions, and the tissues' survival was examined 5 days after thawing (see Figure 7A). We found that a vitrification method with pretreatment in 10% DMSO + 5% ethylene glycol (EG) + 10% sucrose on ice was quite effective for NR cryopreservation not only in terms of tissue survival (Figures 7B and 7C, top row; see the legend for details on epithelial integrity rating), but also for the maintenance of Rx::venus expression (Figure 7C, bottom row and S7A). In contrast, by either criterion, neither the simple one-step vitrification without pretreatment nor the conventional slow-freezing method (with DMSO) was nearly as effective as vitrification with DMSO/EG/sucrose pretreatment (Figures 7B, 7C, and S7A–S7C).

The hESC-derived NR epithelia frozen under the optimized vitrification conditions retained their integrity and semitransparency after freezing and thawing, and grew in the prolonged culture. For instance, the NR epithelia frozen on day 40 uniformly expressed a substantial level of Rx::venus on day 60 (20 days after thawing; Figure 7D). These NR epithelia showed layer formation of Chx10$^+$ progenitors and Pax6$^+$ ganglion cells, and contained Blimp1$^+$ photoreceptor precursors (Figure 7E and 7F and not shown), indicating that the stratified NR tissues had been preserved. The integrity, transparency, and photoreceptor-generating ability (both cones and rods) were kept well even when day-105 NR tissues were cryopreserved (Figures 7G–7I and S7D).

In addition, DAPT treatment of NR epithelia that had been cryopreserved and thawed caused a massive induction of Crx::venus$^+$ photoreceptor precursors (Figure 7J–7L and S7E; in these panels, the NR epithelia were frozen on day 33 and treated with the vehicle DMSO or DAPT during days 38–49).

DISCUSSION

Self-Organization of Optic Cup from hESCs

In this study, we demonstrated that spontaneous emergence of a highly ordered retinal structure (optic cup) occurs in 3D culture of an unpatterned, homogenous aggregate of hESCs. This finding supports the idea that there is a latent intrinsic order for retinal morphogenesis present in early progenitors across species.

In SFEBq culture of hESCs, the combination of early Wnt inhibition, ECM addition, Hedgehog signaling, and FBS treatment strongly promotes the generation of retinal epithelium. Hedgehog signaling may be involved in the adjustment of positional information along the dorsal-ventral axis within hESC-derived forebrain tissue. FBS has also been shown to enhance retinal differentiation from mESCs (Ikeda et al., 2005). Low-molecular-weight factors in FBS do not appear to have a major role, since dialyzed FBS showed a similar activity. The effect of FBS could be not substituted by IGF, Activin, or FGF2 (growth factors implicated for retinal differentiation; data not shown) or by fibronectin or vitronectin (matrix proteins abundantly present in FBS) (Figures S2C–S2F and data not shown).

After the initial retinal specification in these conditions, Wnt augmentation at a specific time window was critical for the balanced generation of both NR and RPE and for the reproducible self-formation of optic cup structures in the hESC culture. The efficient timed control of the canonical Wnt pathway (switching off and on during days 0–12 and day 15–18, respectively) was made possible by applying the chemical antagonist and agonist.

Features Specific to hESC-Derived Optic Cup

The hESC-derived optic cup is substantially larger than the mESC-derived cup. The control mechanism for optic-cup size, which appears to be intrinsic to the retinal epithelium, is a very intriguing topic for future investigation. In addition, the isolated hESC-derived NR, which is thick, has a tissue-intrinsic tendency toward apically convex curvature, which was not observed in the isolated mESC-derived NR (Eiraku et al., 2011). Our previous study pointed out three local mechanical rules in optic cup invagination (relaxation-expansion model; Eiraku et al., 2011, 2012), all of which were also seen in the hESC-derived optic cup: myosin inactivation in NR, the wedge shaping of the hinge, and the tangential NR expansion. The addition of a fourth local rule observed here, the intrinsic apical bending property of human NR, may contribute to the strong deformation of this thick epithelial structure.

One possible mechanism for interpreting this autonomous curvature is that the apical deviation of cell-body positions, which is obvious during invagination only in the hESC-derived NR, could contribute to the preferential apical expansion of the tissue. An alternative possibility is basal narrowing of the NR epithelium (e.g., by basal microfilament contraction), an active role of which has been suggested in previous studies using fish (Martinez-Morales et al., 2009). So far, however, we have failed to observe basally dominant accumulation of actin or pMLC2 in the everting NR (Figure S4F and data not shown). On the other hand, the dependence of the NR eversion on integrin activity suggests an essential role for some basement-membrane-derived polarization signals. In the future, it will be intriguing to investigate whether the integrin-sensitive apical deviation of their cell bodies is caused actively, by nuclear attraction toward the apical direction (e.g., Norden et al., 2009), or passively, by extension of their nuclear-free basal processes in the opposite direction.

An unexpected but intriguing finding, again seen only in hESC culture, was two different positions of Crx$^+$ photoreceptor precursors in the developing NR. In mESC-derived NR, as well

(C) Bright-field and fluorescence views of NR epithelia after cryopreservation under each condition, 5 days after thawing (frozen on day 30).
(D–F) Immunostaining of NR epithelia cryopreserved on day 40 and cultured for an additional 20 days after thawing.
(G–I) Day-126 NR epithelia (carrying *Rx::venus*) frozen on day 105 and fixed on day 126. (G) Low-magnification external view (bright-field and fluorescence). Even after freezing and thawing at this late stage, the tissue kept reasonable semitransparency. (H and I) Immunostaining of sections for Recoverin (H) and Nrl/Rxr-gamma (I).
(J–L) Immunostaining of NR epithelia cryopreserved on day 33 and cultured for an additional 16 days after thawing. Treated with DAPT (L) or DMSO (vehicle; J and K) during days 38–49. Massive induction of Crx::venus$^+$ photoreceptors by DAPT was seen (compare K and L).
Scale bars: 200 μm (C, D, and G); 100 μm (J); 50 μm (H and I). See also Figure S7.

as the mouse embryonic eye, most of the photoreceptor precursors remain in the apical-most zone (Eiraku et al., 2011). In day-34 NR derived from hESCs, early Crx$^+$ photoreceptor precursors were found mostly in the intermediate-deep layer. Substantial numbers of Crx$^+$ photoreceptor precursors were found in both the apical-most and intermediate-deep layers on days 40 and 60. Both populations express Recoverin and are negative for the mitotic marker Ki67, indicating that they, including those in the intermediate-deep zone, are not proliferative progenitors. Later, on days 91–126, Crx$^+$ photoreceptor precursors gradually decrease in number from the intermediate-deep layer, while those in the apical-most layer increase and start expressing rod- or cone-specific markers. At present, the nature of the photoreceptor precursors in the early intermediate-deep layer is unclear, as there has been no previous report describing this ectopic transient population of photoreceptor precursors in the human fetal retina (O'Brien et al., 2003). One obvious question is whether the photoreceptor precursors in the intermediate-deep zone are somewhat less mature than those in the apical-most zone. This could be the case, because the Crx::venus$^+$ cells in the apical-most zone, but not in the intermediate-deep zone, showed a characteristic inner-segment shape with apical junctions and preferentially expressed Nrl and rhodopsin, suggesting a relatively advanced maturation there (Figures 5 and S5). Another open question is whether the population in the intermediate-deep zone comes up to the apical-most zone later, at a certain maturation stage. Above all, it is important to investigate whether the same situation occurs in the early human fetal retina. We think it possible that a similar population exists there, given that such a small, transient population could have been overlooked.

Maturation of hESC-Derived Photoreceptors

The isolated hESC-derived NR epithelia grow well in long-term culture to form stratified NR tissues, which are quite large on day 126 (reaching even 4–5 mm in long-axis diameter). In human fetal development, the generation process of photoreceptors is fairly slow: morphologically recognizable photoreceptors start to appear around fetal week 10 (FW10) at the fovea region (a small central area), and then differentiation very gradually proceeds over the next >15 weeks in the nonfoveal (or noncentral) region, which occupies the majority of the retina (O'Brien et al., 2003; Hendrickson and Provis, 2006). This is in contrast to mouse photoreceptor development, which finishes within 3 weeks after implantation (Graw, 2010). The photoreceptor layer in the hESC-derived NR tissue was relatively sparse with Crx$^+$ cells even on day 60 and became substantially photoreceptor dense only after day 91. In the human fetal retina, Nrl$^+$ rod precursors only gradually increase in number during FW13–19 in the nonfoveal region, while rhodopsin expression is not obviously seen in the majority of the retinal region even in FW19, except in the central-most area including the perifovea and optic-disc regions (O'Brien et al., 2003). Generation of bipolar cells occurs even later, and a long period of culture may be necessary to form fully stratified NR with mature bipolar cells.

Whereas reasonable development of inner segments and connecting cilia was seen in hESC-derived photoreceptors located in the apical-most layer, the formation of obvious outer segments (light-sensing parts) was not clearly observed. Outer-segment development is likely to require further recapitulation of microenvironments that are created by RPE and other intraocular tissues. This is an important future research topic, because successful outer-segment generation could be essential for functional analysis of the hESC-derived NR for light responsiveness.

Toward Future Medical Applications

Practically speaking, however, it may not be necessary to generate all the NR layers through an extremely long culture for regenerative medicine applications. Even if fully mature, stratified NR tissue was available, replacing a patient's retina with full-thickness, hESC-derived retina would be unrealistic, as it is presently too difficult to rewire optic nerves (axons of the grafted ganglion cells) to the brain in adult mammals (MacLaren, 1999). In addition, most types of retinal degeneration (including retinitis pigmentosa) primarily impair photoreceptors (Pennesi et al., 2010; Rivolta et al., 2002). Therefore, as a strategy for retinal degeneration therapy, it seems reasonable to graft hESC-derived NR epithelia just mature enough to carry a large number of photoreceptor precursors. A recent mouse transplantation study strongly supports this direction of general strategy (Pearson et al., 2012). Because a previous mouse study has shown that Nrl$^+$ photoreceptor progenitors have the ability to integrate into the host retina (MacLaren et al., 2006), Nrl$^+$ photoreceptors generated from hESCs in our 3D culture (e.g., on day 126) may be already suitable for transplantation.

In addition, retinal sheet transplantation (fetal NR tissue into the subretinal space) has been effective for tissue replacement and the recovery of visual activity in rodent models for retinal degeneration (Seiler et al., 2010). In this case, the photoreceptors in the graft retina sheet connect to the host ganglion cells via the host NR circuitry. Therefore, it will be important in future investigations to examine whether the same approach is also effective for subretinal graft of hESC-derived NR sheets using primate hosts.

Our en bloc cryopreservation technique substantially facilitates the quality control of the tissue products with validation at intermediate steps. Frozen stocks of NR epithelia may be generated at different time points, depending on the intended purpose. For instance, ganglion cells, which degenerate in glaucoma (Osborne, 2008), are already present at relatively early phases (e.g., day 30). For the storage of ganglion cell progenitors, it would be useful to make frozen stocks of NR at an early culture phase (even before day 30) so that additional short-term culture would generate newly differentiated cells. In contrast, for rod photoreceptors, whose differentiation requires a longer culture period, stocks at later culture phases (e.g., day 40 or even day 105) could be more advantageous. Furthermore, the facilitated generation of photoreceptors by DAPT is also applicable if their robust differentiation from the frozen NR stock is desired at an earlier stage. Considering these points, and with this technique enabling proper validation quality of frozen stocks of differentiating NR tissues, it should be possible to prepare large-scale stocks of reasonably pure NR tissues and to deliver frozen aliquots to multiple institutions for clinical trials.

Generally speaking, contamination with irrelevant cells (in particular, undifferentiated cells, which could cause teratoma)

is a major technical problem in medical applications using stem cell derivatives. A notable practical advantage of the self-formed retinal epithelium described above is that the tissue within the retinal domain is almost pure in composition, with very few nonretinal Rx::venus$^-$ cells. We did not detect any Oct4$^+$ or Nanog$^+$ cells in hESC-derived NR epithelia (n = 30), while DAPT-treated NR tissues formed no teratoma after being grafted into SCID mouse testes, even at a high dose ($\sim$10^6 cells; n = 12). In this respect, another technical advantage of the self-formed retinal epithelium is that it has a high optical transparency, unlike other parts of epithelia in the aggregate, and is easily recognizable for excision, even without fluorescence marking. Furthermore, in the case of NR preparation from the optic-cup-forming culture, the demarcation is even easier because NR epithelium in the optic cup is surrounded by RPE, which becomes readily recognizable after its pigmentation.

In conclusion, this study provides a practical method for creating a versatile resource of 3D human retina tissues that could be used in a wide range of biomedical research areas, including pathogenesis, drug discovery, toxicology, gene-therapy technology, and regenerative medicine. Moreover, these tissues may be useful for the study of the human-specific aspects of eye development; such a study would be difficult to perform without this in vitro system.

EXPERIMENTAL PROCEDURES

Retinal Differentiation from hESCs

Undifferentiated hESCs were maintained and cultured as described (Ueno et al., 2006; Watanabe et al., 2007). For retinal differentiation by SFEBq-MIFS culture, hESCs were dissociated to single cells in TrypLE Express (Invitrogen) containing 0.05 mg/ml DNase I (Roche) and 10 μM Y-27632, and were quickly reaggregated using low-cell-adhesion 96-well plates with V-bottomed conical wells (Figure S1F), which we designed by modifying Sumilon PrimeSurface plate (Sumitomo Bakelite), in retinal differentiation medium (9,000 cells/well, 100 μl) containing 20 μM Y-27632. The retinal differentiation medium was G-MEM supplemented with 20% KSR, 0.1 mM nonessential amino acids, 1 mM pyruvate, 0.1 mM 2-mercaptoethanol, 100 U/ml penicillin, and 100 μg/ml streptomycin. Defining the day on which the SFEBq culture was started as day 0, IWR1e (Merck) was added to culture to final 3 μM from day 0 to day 12. Matrigel (growth-factor-reduced; BD Biosciences) was added from day 2 to day 18. For optimized retinal differentiation, FBS (final 10% v/v), Matrigel (final 1% v/v), and SAG (100 nM, Enzo Life Sciences) were also added to medium.

For optic cup formation, IWR1e was removed from culture by being washed with noncontaining medium on day 12. From day 15 to day 18, 3 μM CHIR99021 (or 40 ng/ml Wnt3a, R&D) and 100 nM SAG (or 100 ng/ml recombinant human Shh, R&D) were added to differentiation medium containing 10% FBS. On day 18, the culture was transferred to an NR culture medium (DMEM/F12-Glutamax medium containing the N2 supplement). Please see Supplemental Experimental Procedures for the details of live imaging, FACS, qPCR, *venus* knockin, immunostaining, and electron microscope and size measurement procedures.

Long-Term NR Culture

NR tissues could be generated under both NR-selective (SFEBq/MIFS) and optic-cup-forming (SFEBq/MIFS+W) conditions (Figures 1 and 2). In both cases, NR epithelia isolated on day 18 or 24 continuously grew under the high-O_2 condition (40%) in retina maturation medium at least for the next several weeks. The NR-selective culture more efficiently generates continuous and large NR tissues in vitro, and was mainly used in the long-term culture study for NR layer formation.

Rx::venus$^+$ retinal epithelium was excised from the main body of the SFEBq aggregate with fine forceps under a dissecting microscope on day 18 and was cultured in suspension (60 NR pieces/10 cm dish for days 18–60; 30 NR pieces after day 60) under 40% O_2/5% CO_2 conditions in DMEM/F12-Glutamax medium (GIBCO) containing the N2 supplement (1×; Invitrogen), 10% FBS, 0.5 μM retinoic acid (Sigma-Aldrich), 0.25 μg/ml Fungizone (GIBCO), 100 U/ml penicillin, and 100 μg/ml streptomycin. For efficiently detecting visual pigments on day 126, retinoic acid (which promotes the growth of NR but tends to delay maturation of photoreceptors; a similar observation has been reported for RPE; Janssen et al., 2000) was removed from culture medium during the last 5 days.

For eversion assay, day-18 Rx::venus$^+$ retinal epithelia generated in the NR-selective hESC culture were excised, and then cultured in suspension as above until day 22. Culture was also treated with a neutralizing antibody against integrin-β1 (IgG1/mouse mAB/Calbiochem; 5 μg/ml) or Y-27632 (10 μM).

Cryopreservation of Neural Retinal Epithelium En Bloc

For cryopreservation of excised NR tissue by vitrification, following the pretreatment, NR tissues (15–20 pieces/condition) were suspended in 200 μl of ice-cold differentiation medium supplemented with 2 M DMSO, 1 M acetamide, and 3 M propylene glycol and were quickly frozen in a 1.5 ml cryogenic tube (Nunc) by directly immersion of the tube in liquid N_2. For pretreatment prior to vitrification, NR tissues were transferred to a 15 ml tube with 1 ml of NR culture medium and kept on ice for 10 min. The supernatant was removed and replaced with a pretreatment solution consisting of NR culture medium containing cryoprotectants (10% DMSO, 5% ethylene glycol, and 10% sucrose) and was kept on ice for 15 to 20 min. After removal of the pretreatment solution, the NR tissues were cryopreserved by vitrification as described above. The frozen NR tissues were thawed quickly by the addition of warmed medium directly to the freezing tube and were recovered for replating. After a 5 day culture of the thawed NR tissues, the epithelial continuity (bright-field images) and Rx::venus expression (fluorescent image) were evaluated using NIH Image J.

SUPPLEMENTAL INFORMATION

Supplemental Information for this article includes seven figures, four movies, and Supplemental Experimental Procedures and can be found with this article online at doi:10.1016/j.stem.2012.05.009.

ACKNOWLEDGMENTS

We are grateful to Masatoshi Ohgushi, Hidetaka Suga, and Taisuke Kadoshima for invaluable comments; Kazuyo Misaki for electron microscopy analysis; Masayo Takahashi and Michiko Mandai for discussion on photoreceptor maturation; and Tadayoshi Ueda for discussion on cryopreservation. This work was supported by grants-in-aid from MEXT (Y.S., M.E., S.Y., and Ki.S.) and the Ministry of Health, Labor, and Welfare (K.M.); the S-Innovation from JST (S.A., Ko.S., Ki.S., and Y.S.); and the Leading Project for Realization of Regenerative Medicine (Y.S.).

Received: November 26, 2011
Revised: March 29, 2012
Accepted: May 4, 2012
Published: June 14, 2012

REFERENCES

Ali, R.R., and Sowden, J.C. (2011). Regenerative medicine: DIY eye. Nature *472*, 42–43.

Besharse, J.C., and Insinna, C. (2010). The photoreceptor outer segment as a sensory cilium. In The Retina and Its Disorder, Second Edition, J.C. Besharse and D. Bok, eds. (Oxford: Academic Press).

Boucherie, C., Sowden, J.C., and Ali, R.R. (2011). Induced pluripotent stem cell technology for generating photoreceptors. Regen. Med. *6*, 469–479.

Brzezinski, J.A., 4th, Lamba, D.A., and Reh, T.A. (2010). Blimp1 controls photoreceptor versus bipolar cell fate choice during retinal development. Development *137*, 619–629.

Carr, A.J., Vugler, A.A., Hikita, S.T., Lawrence, J.M., Gias, C., Chen, L.L., Buchholz, D.E., Ahmado, A., Semo, M., Smart, M.J., et al. (2009). Protective effects of human iPS-derived retinal pigment epithelium cell transplantation in the retinal dystrophic rat. PLoS ONE *4*, e8152.

Cayouette, M., Poggi, L., and Harris, W.A. (2006). Lineage in the vertebrate retina. Trends Neurosci. *29*, 563–570.

Eiraku, M., Watanabe, K., Matsuo-Takasaki, M., Kawada, M., Yonemura, S., Matsumura, M., Wataya, T., Nishiyama, A., Muguruma, K., and Sasai, Y. (2008). Self-organized formation of polarized cortical tissues from ESCs and its active manipulation by extrinsic signals. Cell Stem Cell *3*, 519–532.

Eiraku, M., Takata, N., Ishibashi, H., Kawada, M., Sakakura, E., Okuda, S., Sekiguchi, K., Adachi, T., and Sasai, Y. (2011). Self-organizing optic-cup morphogenesis in three-dimensional culture. Nature *472*, 51–56.

Eiraku, M., Adachi, T., and Sasai, Y. (2012). Relaxation-expansion model for self-driven retinal morphogenesis: a hypothesis from the perspective of bio-systems dynamics at the multi-cellular level. Bioessays *34*, 17–25.

Fuhrmann, S. (2008). Wnt signaling in eye organogenesis. Organogenesis *4*, 60–67.

Fujimura, N., Taketo, M.M., Mori, M., Korinek, V., and Kozmik, Z. (2009). Spatial and temporal regulation of Wnt/beta-catenin signaling is essential for development of the retinal pigment epithelium. Dev. Biol. *334*, 31–45.

Fujitani, Y., Fujitani, S., Luo, H., Qiu, F., Burlison, J., Long, Q., Kawaguchi, Y., Edlund, H., MacDonald, R.J., Furukawa, T., et al. (2006). Ptf1a determines horizontal and amacrine cell fates during mouse retinal development. Development *133*, 4439–4450.

Furukawa, T., Morrow, E.M., and Cepko, C.L. (1997). Crx, a novel otx-like homeobox gene, shows photoreceptor-specific expression and regulates photoreceptor differentiation. Cell *91*, 531–541.

Graw, J. (2010). Eye development. Curr. Top. Dev. Biol. *90*, 343–386.

Hendrickson, A., and Provis, J. (2006). Comparison of development of the primate fovea centralis with peripheral retina. In Retinal Development, E. Sernagor, S. Eglen, B. Harris, and R. Wong, eds. (Cambridge: Cambridge University Press).

Hilfer, S.R., and Yang, J.W. (1980). Accumulation of CPC-precipitable material at apical cell surfaces during formation of the optic cup. Anat. Rec. *197*, 423–433.

Idelson, M., Alper, R., Obolensky, A., Ben-Shushan, E., Hemo, I., Yachimovich-Cohen, N., Khaner, H., Smith, Y., Wiser, O., Gropp, M., et al. (2009). Directed differentiation of human embryonic stem cells into functional retinal pigment epithelium cells. Cell Stem Cell *5*, 396–408.

Ikeda, H., Osakada, F., Watanabe, K., Mizuseki, K., Haraguchi, T., Miyoshi, H., Kamiya, D., Honda, Y., Sasai, N., Yoshimura, N., et al. (2005). Generation of Rx+/Pax6+ neural retinal precursors from embryonic stem cells. Proc. Natl. Acad. Sci. USA *102*, 11331–11336.

Ishikawa, T., and Yamada, E. (1969). Atypical mitochondria in the ellipsoid of the photoreceptor cells of vertebrate retinas. Invest. Ophthalmol. *8*, 302–316.

Jadhav, A.P., Mason, H.A., and Cepko, C.L. (2006). Notch 1 inhibits photoreceptor production in the developing mammalian retina. Development *133*, 913–923.

Janssen, J.J., Kuhlmann, E.D., van Vugt, A.H., Winkens, H.J., Janssen, B.P., Deutman, A.F., and Driessen, C.A. (1999). Retinoic acid receptors and retinoid X receptors in the mature retina: subtype determination and cellular distribution. Curr. Eye Res. *19*, 338–347.

Janssen, J.J., Kuhlmann, E.D., van Vugt, A.H., Winkens, H.J., Janssen, B.P., and Deutman, A.F. (2000). Retinoic acid delays transcription of human retinal pigment neuroepithelium marker genes in ARPE-19 cells. Neuroreport *11*, 1571–1579.

Katoh, K., Omori, Y., Onishi, A., Sato, S., Kondo, M., and Furukawa, T. (2010). Blimp1 suppresses Chx10 expression in differentiating retinal photoreceptor precursors to ensure proper photoreceptor development. J. Neurosci. *30*, 6515–6526.

Kawasaki, H., Suemori, H., Mizuseki, K., Watanabe, K., Urano, F., Ichinose, H., Haruta, M., Takahashi, M., Yoshikawa, K., Nishikawa, S.i., et al. (2002). Generation of dopaminergic neurons and pigmented epithelia from primate ES cells by stromal cell-derived inducing activity. Proc. Natl. Acad. Sci. USA *99*, 1580–1585.

Lamba, D.A., Karl, M.O., Ware, C.B., and Reh, T.A. (2006). Efficient generation of retinal progenitor cells from human embryonic stem cells. Proc. Natl. Acad. Sci. USA *103*, 12769–12774.

Lamba, D.A., McUsic, A., Hirata, R.K., Wang, P.R., Russell, D., and Reh, T.A. (2010). Generation, purification and transplantation of photoreceptors derived from human induced pluripotent stem cells. PLoS ONE *5*, e8763.

Liu, I.S., Chen, J.D., Ploder, L., Vidgen, D., van der Kooy, D., Kalnins, V.I., and McInnes, R.R. (1994). Developmental expression of a novel murine homeobox gene (Chx10): evidence for roles in determination of the neuroretina and inner nuclear layer. Neuron *13*, 377–393.

Liu, W., Lagutin, O., Swindell, E., Jamrich, M., and Oliver, G. (2010). Neuroretina specification in mouse embryos requires Six3-mediated suppression of Wnt8b in the anterior neural plate. J. Clin. Invest. *120*, 3568–3577.

Lu, B., Malcuit, C., Wang, S., Girman, S., Francis, P., Lemieux, L., Lanza, R., and Lund, R. (2009a). Long-term safety and function of RPE from human embryonic stem cells in preclinical models of macular degeneration. Stem Cells *27*, 2126–2135.

Lu, J., Ma, Z., Hsieh, J.C., Fan, C.W., Chen, B., Longgood, J.C., Williams, N.S., Amatruda, J.F., Lum, L., and Chen, C. (2009b). Structure-activity relationship studies of small-molecule inhibitors of Wnt response. Bioorg. Med. Chem. Lett. *19*, 3825–3827.

Lund, R.D., Wang, S., Klimanskaya, I., Holmes, T., Ramos-Kelsey, R., Lu, B., Girman, S., Bischoff, N., Sauvé, Y., and Lanza, R. (2006). Human embryonic stem cell-derived cells rescue visual function in dystrophic RCS rats. Cloning Stem Cells *8*, 189–199.

MacLaren, R.E. (1999). Re-establishment of visual circuitry after optic nerve regeneration. Eye (Lond.) *13* (Pt 3a), 277–284.

MacLaren, R.E., Pearson, R.A., MacNeil, A., Douglas, R.H., Salt, T.E., Akimoto, M., Swaroop, A., Sowden, J.C., and Ali, R.R. (2006). Retinal repair by transplantation of photoreceptor precursors. Nature *444*, 203–207.

Martínez-Morales, J.R., Rodrigo, I., and Bovolenta, P. (2004). Eye development: a view from the retina pigmented epithelium. Bioessays *26*, 766–777.

Martinez-Morales, J.R., Rembold, M., Greger, K., Simpson, J.C., Brown, K.E., Quiring, R., Pepperkok, R., Martin-Bermudo, M.D., Himmelbauer, H., and Wittbrodt, J. (2009). ojoplano-mediated basal constriction is essential for optic cup morphogenesis. Development *136*, 2165–2175.

Mathers, P.H., Grinberg, A., Mahon, K.A., and Jamrich, M. (1997). The Rx homeobox gene is essential for vertebrate eye development. Nature *387*, 603–607.

Mears, A.J., Kondo, M., Swain, P.K., Takada, Y., Bush, R.A., Saunders, T.L., Sieving, P.A., and Swaroop, A. (2001). Nrl is required for rod photoreceptor development. Nat. Genet. *29*, 447–452.

Meyer, J.S., Howden, S.E., Wallace, K.A., Verhoeven, A.D., Wright, L.S., Capowski, E.E., Pinilla, I., Martin, J.M., Tian, S., Stewart, R., et al. (2011). Optic vesicle-like structures derived from human pluripotent stem cells facilitate a customized approach to retinal disease treatment. Stem Cells *29*, 1206–1218.

Mu, X., and Klein, W.H. (2004). A gene regulatory hierarchy for retinal ganglion cell specification and differentiation. Semin. Cell Dev. Biol. *15*, 115–123.

Norden, C., Young, S., Link, B.A., and Harris, W.A. (2009). Actomyosin is the main driver of interkinetic nuclear migration in the retina. Cell *138*, 1195–1208.

O'Brien, K.M., Schulte, D., and Hendrickson, A.E. (2003). Expression of photoreceptor-associated molecules during human fetal eye development. Mol. Vis. *9*, 401–409.

O'Rahilly, R., and Müller, F. (1999). The Embryonic Human Brain, Second Edition (New York: Willy-Liss), pp. 129–138.

Ohgushi, M., Matsumura, M., Eiraku, M., Murakami, K., Aramaki, T., Nishiyama, A., Muguruma, K., Nakano, T., Suga, H., Ueno, M., et al. (2010). Molecular pathway and cell state responsible for dissociation-induced apoptosis in human pluripotent stem cells. Cell Stem Cell *7*, 225–239.

Osakada, F., Ikeda, H., Mandai, M., Wataya, T., Watanabe, K., Yoshimura, N., Akaike, A., Sasai, Y., and Takahashi, M. (2008). Toward the generation of rod

and cone photoreceptors from mouse, monkey and human embryonic stem cells. Nat. Biotechnol. *26*, 215–224.

Osborne, N.N. (2008). Pathogenesis of ganglion "cell death" in glaucoma and neuroprotection: focus on ganglion cell axonal mitochondria. Prog. Brain Res. *173*, 339–352.

Pearson, R.A., Barber, A.C., Rizzi, M., Hippert, C., Xue, T., West, E.L., Duran, Y., Smith, A.J., Chuang, J.Z., Azam, S.A., et al. (2012). Restoration of vision after transplantation of photoreceptors. Nature *485*, 99–103.

Pennesi, M.E., Francis, P.J., and Weleber, R.G. (2010). Primary Photoreceptor degeneration: retinitis pigmentosa. In The Retina and Its Disorder, Second Edition, J.C. Besharse and D. Bok, eds. (Oxford: Academic Press).

Rivolta, C., Sharon, D., DeAngelis, M.M., and Dryja, T.P. (2002). Retinitis pigmentosa and allied diseases: numerous diseases, genes, and inheritance patterns. Hum. Mol. Genet. *11*, 1219–1227.

Seiler, M.J., Aramant, R.B., Thomas, B.B., Peng, Q., Sadda, S.R., and Keirstead, H.S. (2010). Visual restoration and transplant connectivity in degenerate rats implanted with retinal progenitor sheets. Eur. J. Neurosci. *31*, 508–520.

Ueno, M., Matsumura, M., Watanabe, K., Nakamura, T., Osakada, F., Takahashi, M., Kawasaki, H., Kinoshita, S., and Sasai, Y. (2006). Neural conversion of ES cells by an inductive activity on human amniotic membrane matrix. Proc. Natl. Acad. Sci. USA *103*, 9554–9559.

Watanabe, K., Ueno, M., Kamiya, D., Nishiyama, A., Matsumura, M., Wataya, T., Takahashi, J.B., Nishikawa, S., Nishikawa, S., Muguruma, K., and Sasai, Y. (2007). A ROCK inhibitor permits survival of dissociated human embryonic stem cells. Nat. Biotechnol. *25*, 681–686.

Wataya, T., Ando, S., Muguruma, K., Ikeda, H., Watanabe, K., Eiraku, M., Kawada, M., Takahashi, J., Hashimoto, N., and Sasai, Y. (2008). Minimization of exogenous signals in ES cell culture induces rostral hypothalamic differentiation. Proc. Natl. Acad. Sci. USA *105*, 11796–11801.

Westenskow, P., Piccolo, S., and Fuhrmann, S. (2009). Beta-catenin controls differentiation of the retinal pigment epithelium in the mouse optic cup by regulating Mitf and Otx2 expression. Development *136*, 2505–2510.